Horn Antenna Development at 80 GHz for Tank Level Probing Radar Applications

Lajos Nagy, *Member, IEEE*

***Abstract*—One important application and research area of radar technology is tank-level measurement and detection. Radar contactless level measurement is a safe solution even in extreme process conditions, such as significant overpressure, high temperatures, and the presence of corrosive vapors. The main categories of these principles are ultrasonic, and electromagnetic wave radars.**

We will now consider only radars using electromagnetic waves. The use of millimeter radio waves, which we use, is nowadays becoming more and more common also for automotive radars, human presence detection and human vital signs.

To meet electromagnetic requirements such as high gain, low spurious levels, and high bandwidth, special antennas are required.

The low sidelobe level and narrow main beam mainly reduce reflections from the side of the tank while the bandwidth determines the distance resolution of the measurement system. A further requirement is the small size and reliable manufacturability of the antenna. In the presence of corrosive vapors, antennas must be resistant to corrosion.

The article briefly summarizes the material parameter measurements required for the design of the radar, and the design of the main components. We analyzed the possible dielectric materials that can be used as random or dielectric lenses for such antennas. In the next part of the paper, we present a conical horn antenna design for the 80 GHz band and compare the parameters of an open horn antenna with those of a horn antenna with a dielectric lens. Finally, a tank-level radar designed with the Texas Instruments IWR1443 radar chip is presented.

***Index Terms*—Radar, antenna**

I. Introduction

Product quality control, production safety, and process economy can only be guaranteed can only be ensured by continuous measurements and the monitoring and intervention systems based on them. The main fields of application are the oil industry, petrochemical industry, chemical industry, food industry, pharmaceutical industry, transport, wastewater storage and treatment. Liquids, pastes, bulk solids, and liquefied gases are most stored in tanks, silos, or mobile containers.

Lajos Nagy, is with Budapest University of Technology and Economics, Budapest, Hungary, Department of Broadband Infocommunications and Electromagnetic Theory, Faculty of Electrical Engineering (E-mail: nagy.lajos@vik.bme.hu).

There are several classical and modern methods for measuring the product level in process and storage tanks. Such systems use microwave contactless radar, guided microwave radar, capacitive, magnetostrictive, and ultrasonic sensors.

Antennas for contactless microwave sensors are microstrip antenna systems, horn antennas, dielectric antennas, and slot antennas on waveguides.

Applications are in the chemical, petrochemical, pharmaceutical, water, and food industries, mobile tanks on vehicles and ships, and natural reservoirs such as seas, dams, lakes, and oceans. Typical tank heights for these applications are in the range of 0.5 m to 37 m.

In practical applications, two main measurement tasks can be distinguished:

- continuous level measurement, i.e., level indication,
- level detection, i.e., detection of an alarm limit to prevent overfilling.

Many level measurement devices are mounted on top of the tank and measure primarily the distance between their mounting position and the product's surface (Fig. 1).

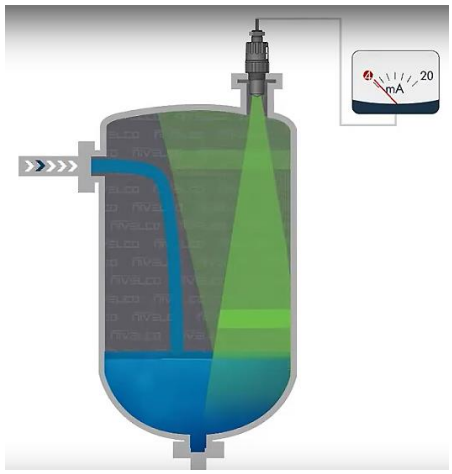

Fig. 1. Tank with liquid and non-contact sensors on the top of the tank

The sensor is placed in an opening on the top surface of the tank. As shown in the figure, the position of the sensor must be shifted laterally due to the fluid flowing through the inlet. This in turn causes reflections and consequently multiple reflections and makes level measurement difficult. (Fig. 1.)

DOI: 10.36244/ICJ.2025.1.4

Fig. 2. Horn antenna with house contains signal processing and communications circuits.

A typical horn antenna design is shown in Figure 2. The diameter of the antenna must be adapted to the size of the tank's opening to allow installation of the antenna.

For level measurement, a significant number of different principles measurement techniques are available [1,2], and it is advisable to select the optimum technique and sensor.

There is a recent trend for contactless radio sensors to operate in the increasingly higher microwave band.

Radio regulations distinguish between "tank level probing radar" inside closed metallic tanks or silos and "level probing radar" outside with more restrictions.

Tank Level Probing Radar (TLPR) applications are based on pulse RF, FMCW, or similar wideband techniques. TLPR radio equipment types can operate in all or part of the frequency bands as specified in Table I.

TABLE I
TANK LEVEL PROBING RADAR (TLPR) PERMITTED FREQUENCY BANDS [3]

	TLPR assigned frequency bands (GHz)
Transmit and receive	4,5 to 7
Transmit and receive	8,5 to 10,6
Transmit and receive	24,05 to 27
Transmit and receive	57 to 64
Transmit and receive	75 to 85

For aperture antennas, there is a clear relationship between the geometrical area of the aperture and the effective aperture area. This relationship is the aperture efficiency, which is typically between 0.4-0.7. The operating free-space wavelength gives the relationship between effective aperture area and antenna gain.

$$A_{geom}\eta_A = A_{eff} = \frac{\lambda^2}{4\pi}G \quad (1)$$

where

G the antenna gain,
A_{geom} the geometrical area of the aperture,
η_A aperture efficiency,
A_{eff} effective aperture area
λ operating free space wavelength.

For antennas considered lossless, the gain of the antennas can be expressed in terms of the main beam cone angle.

$$G \approx \frac{16}{\Theta^2} \quad (2)$$

where
Θ the antenna main beam cone angle.

It is easy to see from equations (1) and (2) that for the same aperture geometrical area, the main beam cone angle of the antenna decreases with increasing frequency.

$$\Theta \sim \lambda = \frac{c}{freq} \quad (3)$$

where
$freq$ operating frequency,
c the speed of light in a vacuum.

From the relationship in equation (3), it is clear, that for the same antenna aperture size, as the frequency increases, the beamwidth decreases, and the narrower antenna foot reduces the reflection from the tank sides. In addition, increasing the frequency has the further advantage of improving the radar distance measurement resolution and reducing the circuit dimensions. For these reasons we have chosen the 75-85 GHz frequency band from the allocated TLPR bands. [18, 19]

From relation (3), the main beam widths at 25 and 80 GHz can be compared. (Fig. 3)

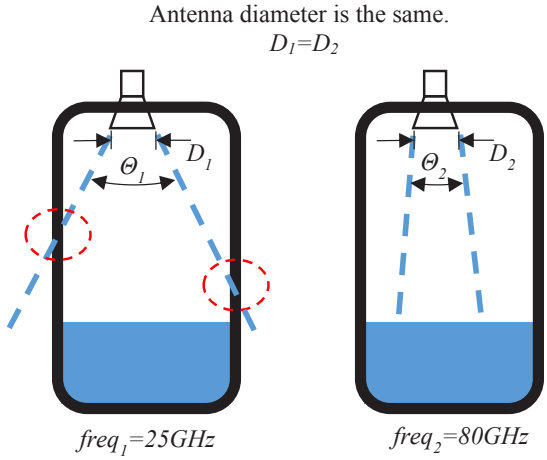

Fig. 3. Measurement in narrow tanks or silos [4]

In practice, the footprint size is often used to compare the size of the tank or silo and the main beam at each frequency. (Fig. 4.) The simulation parameters are aperture geometrical area 0.01m^2, aperture efficiency 0.6, distance 10m.

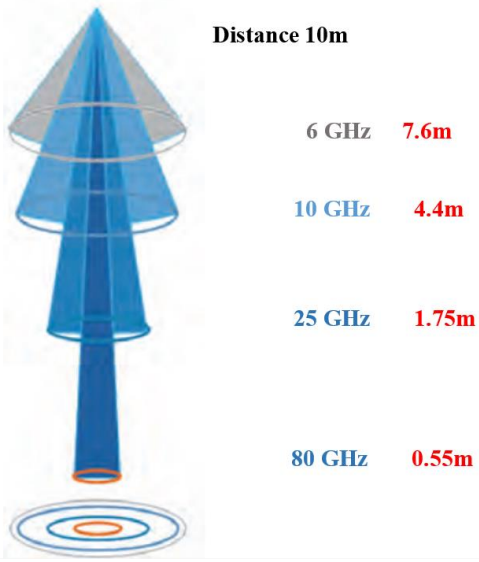

Fig. 4. Antenna footprint diameters for different frequencies

In summary, the antenna radiation field is inversely proportional to the aperture diameter of the antenna and the center frequency. Beam width decreases with increasing center frequency if the diameter of the antenna is kept constant. Furthermore, in the case of keeping the frequency constant, the beam width also decreases with the increasing diameter of the antenna. In conclusion, the beam width does not simply depend on one single parameter, but both parameters—center frequency and antenna diameter are degrees of freedom for determining the angular beam width. The choice of one specific antenna from a set of available antennas with different beam widths must be made dependent on the given application conditions.

II. Dielectric Materials and Permittivity Measurements

The most common plastic materials used as radomes and dielectric lenses for antennas are Polypropylene (PP), Polyvinylidene Fluoride (PVDF), and Polytetrafluoroethylene (PTFE). The electrical parameters, permittivity, and loss of these materials are examined below.

II.1 Dielectric materials

Polypropylene (PP) is one of the most widely used and low-cost thermoplastics with adequate physical properties, such as low density and high heat resistance [5]. PP is generally found as a homopolymer and copolymer. The first one consists of propylene monomers, and it has a high strength-to-weight ratio and good chemical resistance. The second one includes monomers in the PP backbone, and it is tougher and more flexible, with a lower melting point and high-impact resistance at low temperatures than PP homopolymer [6]. Because of all these advantages, polypropylene-based composites have been extensively used for automotive, construction, and packaging applications.

Polyvinylidene fluoride (PVDF) is a highly non-reactive and pure thermoplastic fluoropolymer material. Below 150 ºC, PVDF becomes ferroelectric. Thus, PVDF is an electroactive and semicrystalline polymer with pyro and piezoelectric properties at room temperature, which can be used for many applications [7]. It exhibits high mechanical strength, good chemical resistance, thermal stability, and excellent aging resistance [8]. Moreover, PVDF is an attractive polymer matrix for composite material with superior mechanical and electrical properties.

Polytetrafluoroethylene (FTFE) is a synthetic fluoropolymer of tetrafluoroethylene and is a PFAS that has numerous applications. The commonly known brand name of PTFE-based composition is Teflon. Polytetrafluoroethylene is a fluorocarbon solid, as it is a high-molecular-weight polymer consisting wholly of carbon and fluorine. PTFE is hydrophobic: neither water nor water-containing substances wet PTFE, as fluorocarbons exhibit only small London dispersion forces due to the low electric polarizability of fluorine. PTFE has one of the lowest coefficients of friction of any solid. PTFE is used as a non-stick coating for pans and other cookware. It is non-reactive, partly because of the strength of carbon–fluorine bonds, so it is often used in containers and pipework for reactive and corrosive chemicals. When used as a lubricant, PTFE reduces friction, wear, and energy consumption of machinery.

In the literature [9], the electrical properties of materials are generally known at lower frequencies (1 kHz, 1 MHz), and some materials are manufactured in several versions, so it is necessary to carry out measurements that give the electrical properties of materials in the millimeter waveband.

TABLE II
Electrical Properties of Plastic Materials [9]

Material	Dielectric constant @1MHz	Dissipation factor @ 1MHz	Volume resistivity Ohm/cm
PP	2.2-2.6	0.0003 - 0.0005	10^{16} -10^{18}
PVDF	8.4	0.06	10^{14}
PTFE	2.0-2.1	0.0003 - 0.0007	10^{18} -10^{19}

In the following, such a measurement procedure is presented and the results of electrical parameter measurements for the three materials are reported.

II.2 Material Parameter Measurements

In practice, microwave measurements of electrical material parameters are based on transmission and reflection measurements. (Fig. 5.) [10,11]

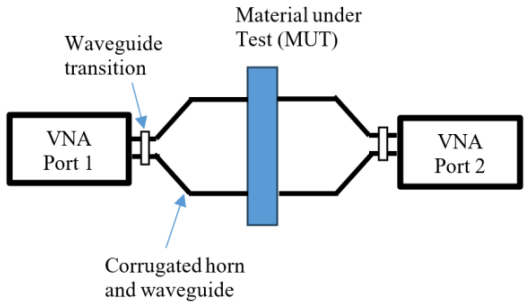

Fig. 5. Measurement set-up for transmission and reflection measurements of electrical material parameters.

According to the setup shown in Figure 5, the material parameter measurement is performed with 2 ports Vector Network Analyzer, and the sample is placed between two corrugated horn antennas for measurement. Properly sized corrugated horn antennas provide plane-wave excitation for the sample.

Measurements are preferably carried out using the Swissto12 Material Characterization Kit (MCK). (Fig. 6.) MCKs are used for measurement of the permittivity and loss tangent of planar specimens, foams, and multilayered materials at room temperature. The MCKs are available to cover the frequency range 50 GHz to 750 GHz.

Fig. 6. Measurement set-up with Swissto12 MCK and Vector Network Analyzer.

To model the measurements, a microwave signal flow graph network model of the measurement setup is presented. (Fig. 7.) [12-14]

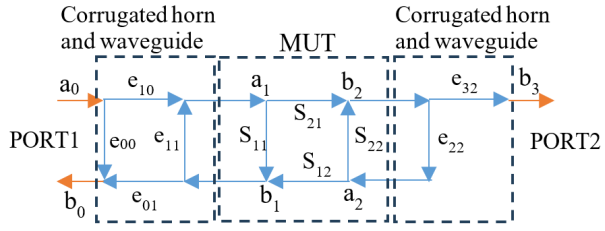

Fig. 7. Microwave signal flow graph of the measurement setup

The VNA measures the reflection and transmission between PORT1 and PORT2.

We introduce the evaluation of transmission parameters from signal flow graph of the measurement setup. The equations below can be used to express the transmission between PORT1 and PORT2.

$$e_{10}a_0 + e_{11}b_1 = a_1$$
$$S_{11}a_1 + S_{12}a_2 = b_1$$
$$S_{21}a_1 + S_{22}a_2 = b_2$$
$$b_3 = e_{32}b_2$$
$$e_{22}b_2 = a_2$$

The measured $S_{m,21}$ parameter $S_{m,21} = b_3/a_0$ can be expressed as.

$$\frac{b_3}{a_0} = \frac{S_{21}e_{10}e_{32}}{1 - S_{11}e_{11} - S_{22}e_{22} + e_{11}e_{22}(S_{11}S_{22} - S_{12}S_{21})}$$

The measured $S_{m,11}$ parameter $S_{m,11} = b_0/a_0$ can be similarly expressed.

Finally, the permittivity and loss factor of the sample are calculated from the S_{ij} scattering coefficients of the MUT.

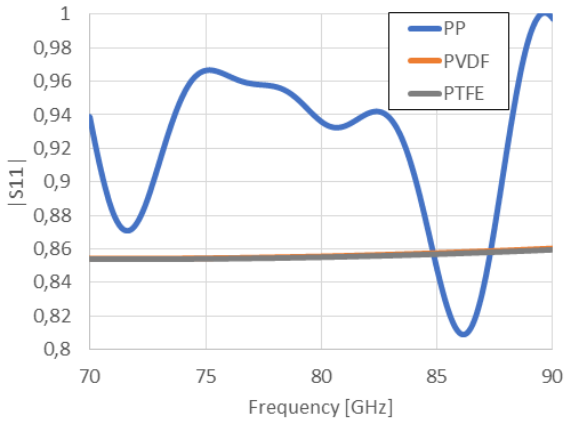

Fig. 8. Measured reflection parameters for PP, PVDF and PTFE samples.

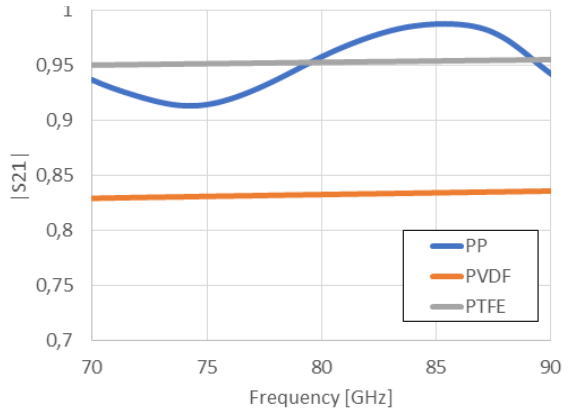

Fig. 9. Measured transmission parameters for PP, PVDF and PTFE samples.

The two material parameters (permittivity and loss tangent) for dielectric materials can be evaluated using S_{11} and S_{21}. These are introduced for PP, PVDF and PTFE in Figure 10 and 11.

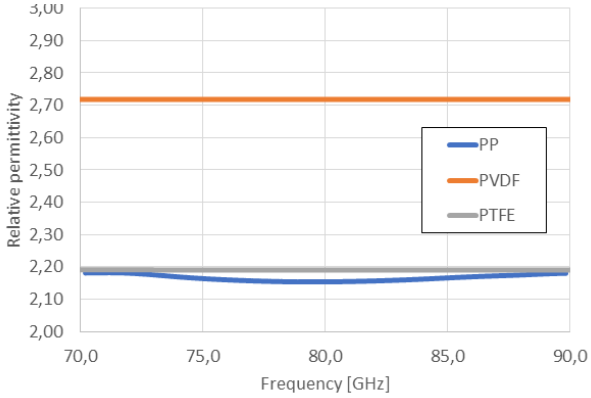

Fig. 10. Relative permittivity for PP, PVDF and PTFE samples.

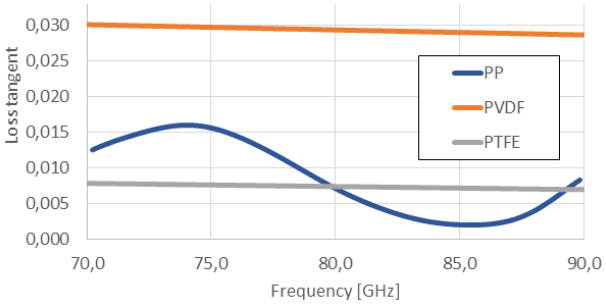

Fig. 11. Loss tangent for PP, PVDF and PTFE samples.

From the measurement results it can be concluded that the permittivity of PTFE can be considered constant over the entire frequency range investigated, and its loss factor is also essentially constant and can be the lowest.

For the horn antenna design with a dielectric lens, we use PTFE in the next sessions.

III. Single Chip Integrated FMCW Radar IWR1443

The IWR1443 device [15, 20] is an integrated single-chip millimeter wave (mmWave) sensor based on FMCW radar technology capable of operation in the 76- to 81 GHz band with up to 4 GHz continuous chirp. The device is built with TI's low-power 45-nm RFCMOS process, and this solution enables unprecedented levels of integration in a tiny form factor. The IWR1443 is an ideal solution for low-power, self-monitored, ultra-accurate radar systems in industrial applications such as building automation, factory automation, drones, material handling, traffic monitoring, and surveillance. The IWR1443 device is a self-contained, single-chip solution that simplifies the implementation of mmWave sensors in the 76 to 81 GHz band. The IWR1443 includes a monolithic implementation of a 3TX, 4RX system with built-in PLL and A2D converters. The device includes fully configurable hardware accelerator that supports complex FFT and CFAR detection. Additionally, the device includes two ARM R4F-based processor subsystems: one processor subsystem is for master control, and additional algorithms; a second processor subsystem is responsible for front-end configuration, control, and calibration. Simple programming model changes can enable a wide variety of sensor implementations with the possibility of dynamic reconfiguration for implementing a multimode sensor.

Automotive radar applications use generally all three Tx and four Rx channels for radar imaging but for our tank-level radar only one Tx and one Rx channels we apply.

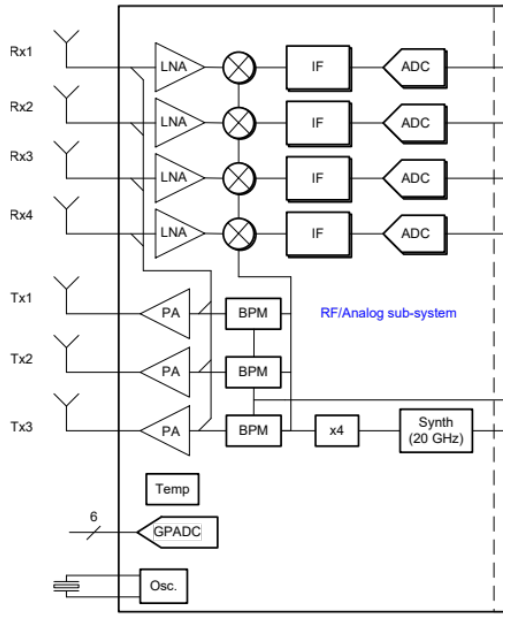

Fig. 12. RF sub-system functional block diagram of IWR1443 [15].

The Fig. 13. shows demo layout of IWR1443 chip with microstrip transmit and receive antennas.

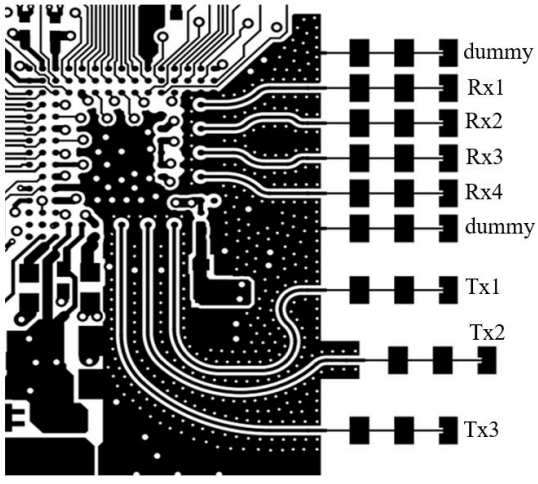

Fig. 13. FMCW radar layout (IWR1443BOOST) using IWR1443 [16].

Fig. 14 shows the main parameters of the antenna. The antenna gain, G=9.59dB, half power conical beam angle, Θ_{3dB}=25 degrees, sidelobe suppression ratio, SLSR=26dB.

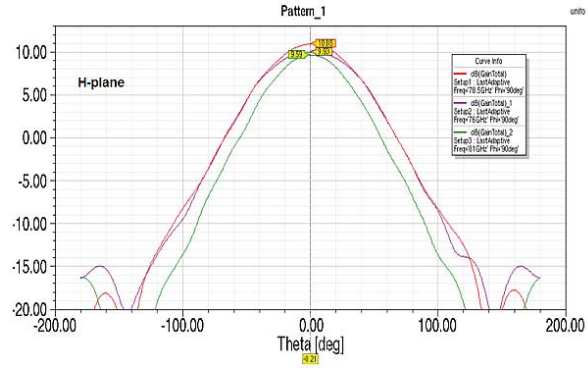

Fig. 14. Microstrip antenna radiation pattern for IWR1443BOOST Evaluation Module [16].

For the planned radar, the microstrip antennas of the IWR1443BOOST demo board cannot be used and new antenna should be designed for the next reasons.

The antenna gain should be increased, and conical beam angle should be decreased to suppress multiple reflections.

The antenna chosen for the design must also be resistant to pressure and corrosive humid media.

Due to these requirements, the antenna type chosen for the analysis was a conical horn antenna. Two types were investigated, the open horn antenna and the closed horn antenna with dielectric lens.

IV. Horn Antenna Design

Cross-sectional images of the analyzed horn antennas are shown in Figure 15 and 16. The material used for the lens was PTFE, which was found to be the best material based on a material parameter test in II. section.

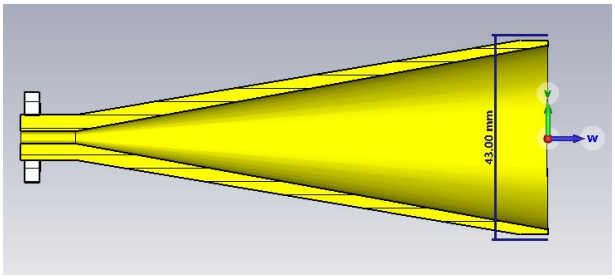

Fig. 15. Cross-sectional image of the analyzed open horn antenna.

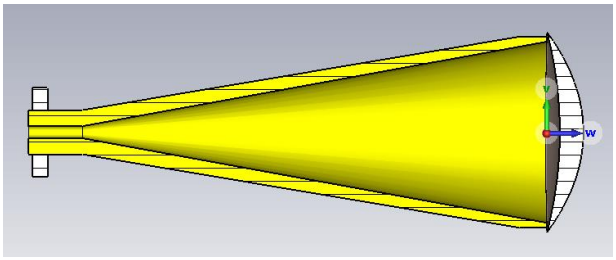

Fig. 16. Cross-sectional image of the analyzed closed horn antenna with dielectric lens.

The simulations were performed using the CST MWS electromagnetic field simulator and the results of the two main simulations (input reflection and radiation pattern) are shown in Figures 17 and 18.

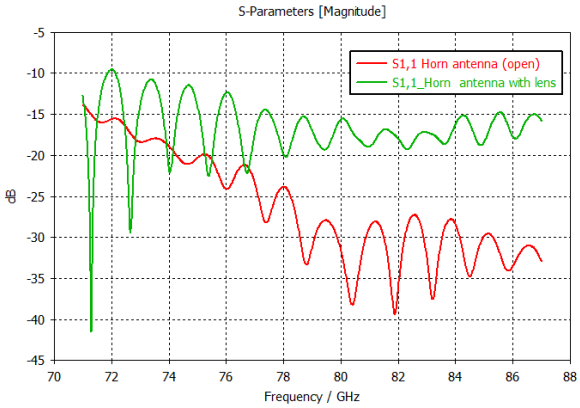

Fig. 17. Input reflection of the horn antennas.

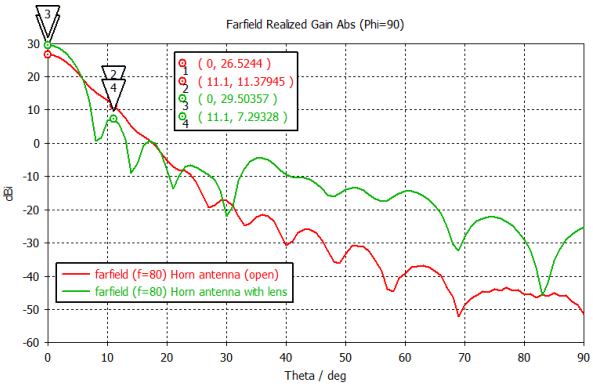

Fig. 18. Radiation pattern of the horn antennas.

The design requirement for input reflection generally below -10 dB, so each of the assumed antennas fulfill that. The antenna gain is optimized using lens on horn aperture and the gain is G=29.5dB. The half power conical beam angle, Θ_{3dB}=6 degrees.

V. Ring Hybrid Design

In radar technology, hybrid ring duplexers often are transmit/receive (TR) switch based on a simple rat-race coupler.

The rat-race coupler has four ports, each placed one-quarter wavelength away from each other around the top half of the ring. (Fig. 19.) A signal input on port 1 will be split between ports 2 and 4, and port 3 will be isolated. [17]

The full simulation has been performed for all gate input reflections and transmissions between gates. Of these, only the simulation results for the transmission between ports 2-3 and port 3 input reflections are reported for different ring radius r=0.5, 0.55 and 0.6 mm. (Fig. 20 and 21)

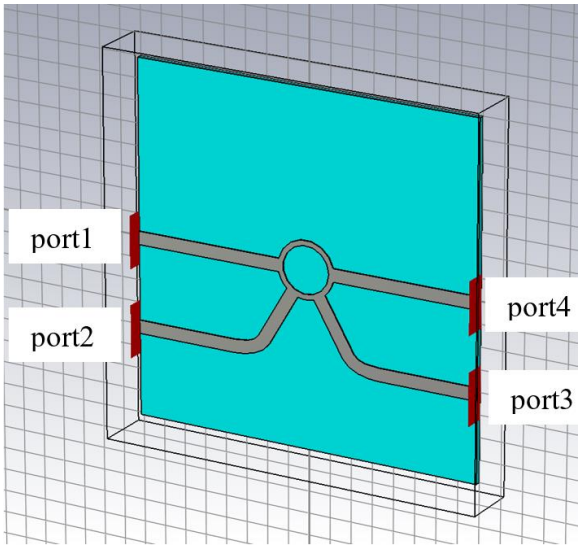

Fig. 19. Rat-race coupler CST simulation model.

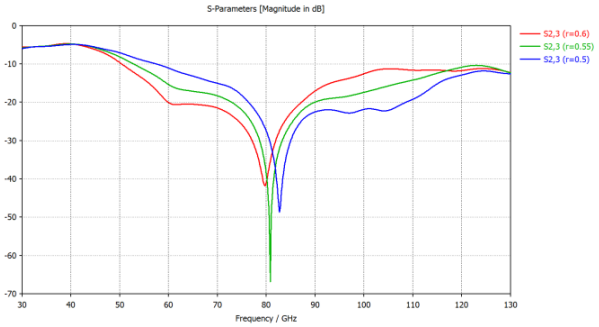

Fig. 20. Rat-race coupler isolation between port 2 and 3 (CST simulation).

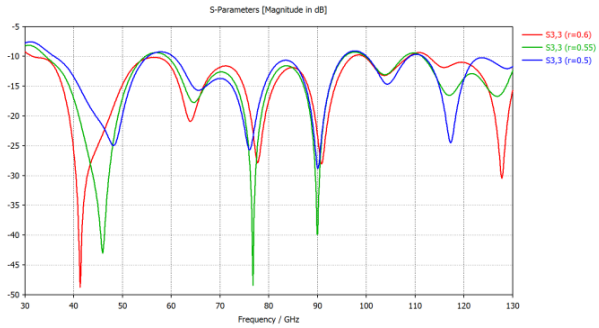

Fig. 21. Rat-race coupler input reflection for port 3 (CST simulation).

The RX1 port is used for reception, while the RX2 port is only used as a matched termination. The TX1 port of the chip's transmit channels is used. (Fig. 22 and 23.)

The radar sensor was tested with a flat target surface. The range-profile characteristics are shown in Fig. 24. for a target with distance of 22m.

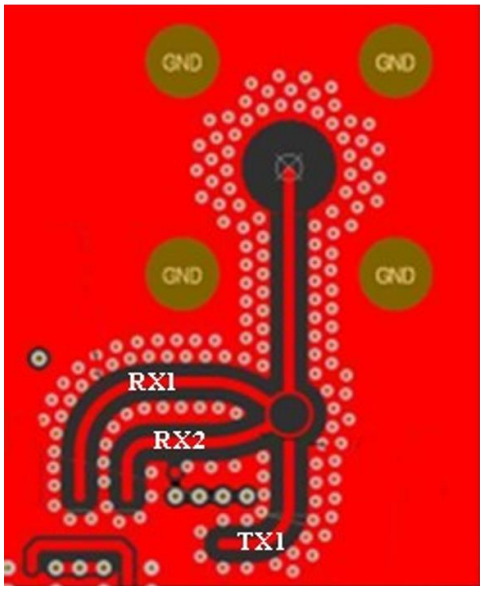

Fig. 22. Rat-race coupler in the radar layout.

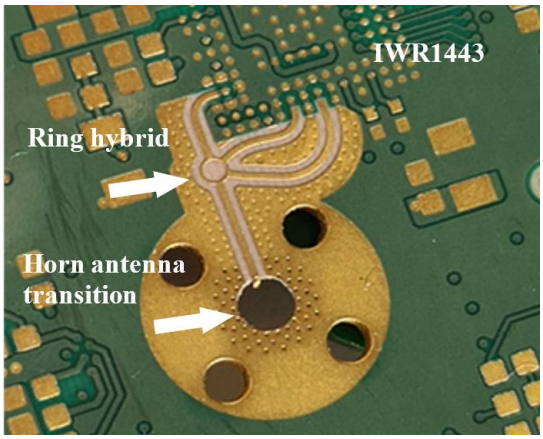

Fig. 23. Rat-race coupler and microstrip-conical waveguide transition.

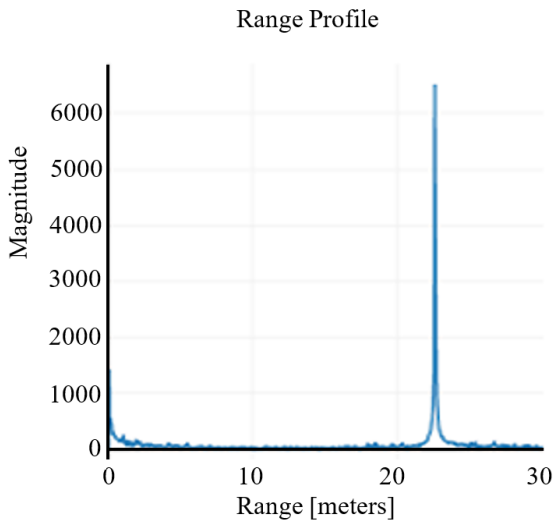

Fig. 24. Measured range-profile characteristics.

VI. SUMMARY

We presented a new systematic design of an 80 GHz radar sensor for contactless tank-level measurement. The reason for choosing this frequency band, mainly to reduce the main beamwidth of the antenna, has been presented. Detailed analysis of possible lens dielectric materials, horn antenna design results and ring hybrid for transmit-receive separation are introduced.

Layout of the antenna and the implemented tank level radar is introduced. Finally, field test was performed, and the measured range-profile test result is presented for the radar to demonstrate the correct functioning of the design.

As a continuation of this work, we plan to increase the range of radar measurements, both near and far.

ACKNOWLEDGMENT

The author very much appreciates the support from the NIVELCO Process Control Co. and the infrastructure of the Department of Broadband Infocommunication and Electromagnetic Theory at the Budapest University of Technology and Economics. The measurements were carried out in Karlsruhe at Karlsruhe Institute of Technology (KIT) at Höchstfrequenztechnik und Elektronik.

This research was funded by the Hungarian Fund 2020-1.1.2-PIACI-KFI-2021-00278.

REFERENCES

[1] Vogt, M., Michael, G.: Silo and tank vision: applications, challenges, and technical solutions for radar measurement of liquids and bulk solids in tanks and silos. *IEEE Microw. Mag*. 18(6), 38–51 (2017)

[2] Vass, Gergely. "The Principles of Level Measurement RF capacitance, conductance, hydrostatic tank gauging, radar, and ultrasonics are the leading sensor technologies in liquid level tank measurement and control operations." Sensors 17 (2000): 55-64.

[3] ETSI EN 302 372, ETSI EN 302 372 V2.1.1 (2016-12), Short Range Devices (SRD); Tank Level Probing Radar (TLPR) equipment operating in the frequency ranges 4,5 GHz to 7 GHz, 8,5 GHz to 10,6 GHz, 24,05 GHz to 27 GHz, 57 GHz to 64 GHz, 75 GHz to 85 GHz; Harmonised Standard covering the essential requirements of article 3.2 of the Directive 2014/53/EU, https://cdn.standards.iteh.ai/samples/46667/1fb304055d624fa1925191db920c0351/ETSI-EN-302-372-V2-1-1-2016-12-.pdf

[4] Dave Grumney, Understanding Radar Technology for Measuring Tank Level, InTech e-edition covering the fundamentals of automation, MARCH 2020, https://www.automation.com/getmedia/6d1ad741-4eb3-450f-9084-7833c2e46105/InTechFOCUS-march2020.pdf

[5] Gogoi R, Kumar N, Mireja S, Ravindranath SS, Manik G, Sinha S. Effect of hollow glass microspheres on the morphology, rheology and crystallinity of short Bamboo fiber-reinforced hybrid polypropylene composite. Journal of Metals. 2019;71(2):548-558. DOI: 10.1007/s11837-018-3268-3

[6] Gogoi R, Maurya AK, Manik G. A review on recent development in carbon fiber reinforced polyolefin composites. Composites Part C: Open Access. 2022;8:100279. DOI: 10.1016/j.jcomc.2022.100279

[7] Zhen Y, Arredondo J and Zhao G 2013 Open Journal of Organic Polymer Materials 3 99

[8] Kang G D and Cao Y M, Application and modification of poly(vinylidene fluoride) (PVDF) membranes – A review 2014 J. Membr. Sci. 463 145

[9] https://www.professionalplastics.com/professionalplastics/ElectricalPropertiesofPlastics.pdf

[10] James Baker Jarvis, Transmission/ Reflection and Short-Circuit Line Methods for Measuring Permittivity and Permeability, *NIST Technical Note* 1341, 1990. https://nvlpubs.nist.gov/nistpubs/Legacy/TN/nbstechnicalnote1341.pdf

[11] Alireza Kazemipour *et. al*., Analytical Uncertainty Evaluation of Material Parameter Measurements at THz Frequencies, *International Journal of Infrared and Millimeter Waves*, 24 July 2020. DOI: 10.1007/s10762-020-00723-0

[12] Alexandros I. Dimitriadis, Dielectric Measurements at mm-Wave Frequencies with the Material Characterization Kit (MCK), Towards Terahertz Technology for High Throughput Communications, EPFL, Lausanne, 5-7 February 2020

[13] A. Kazemipour *et al*., "Standard Load Method: A New Calibration Technique for Material Characterization at Terahertz Frequencies," in *IEEE Transactions on Instrumentation and Measurement*, vol. 70, pp. 1–10, 2021, Art no. 1007310, DOI: 10.1109/TIM.2021.3077660.

[14] Y. Wang *et al*., "Material Measurements Using VNA-Based Material Characterization Kits Subject to Thru-Reflect-Line Calibration," in *IEEE Transactions on Terahertz Science and Technology*, vol. 10, no. 5, pp. 466–473, Sept. 2020, DOI: 10.1109/TTHZ.2020.2999631.

[15] IWR1443 Single-Chip 76- to 81-GHz mmWave Sensor, SWRS211C – MAY 2017 – REVISED OCTOBER 2018 https://www.ti.com/lit/ds/symlink/iwr1443.pdf

[16] IWR1443BOOST Evaluation Module mmWave Sensing Solution, SWRU518D – May 2017 – Revised May 2020 https://www.ti.com/lit/ug/swru518d/swru518d.pdf

[17] Microstrip Hybrid Ring Coupler. Patent, Accession Number: ADD005347, 1978-06-06, https://apps.dtic.mil/sti/citations/ADD005347

[18] Tim Erich Wegner *et. al*., Fill level measurement of low-permittivity material using an M-sequence UWB radar, *International Journal of Microwave and Wireless Technologies* , Volume 15 , Special Issue 8: EuCAP 2022 Special Issue , October 2023, pp. 1299–1307

[19] I. Ullmann, R. G. Guendel, N. C. Kruse, F. Fioranelli and A. Yarovoy, "A Survey on Radar-Based Continuous Human Activity Recognition," in *IEEE Journal of Microwaves*, vol. 3, no. 3, pp. 938–950, July 2023

[20] Li, B.Y., Ding, S.Y., Ma, D., Wu, Y.X., Liao, H.J. and Hu, K.Y. (2024) LLMCount: Enhancing Stationary mmWave Detection with Multimodal-LLM. https://arxiv.org/abs/2409.16209

Lajos Nagy He received the Engineer option Communication) and PhD degrees, both from the Budapest University of Technology and economics (BME), Budapest, Hungary, in 1986 and 1995, respectively. He joined the department of Microwave Telecommunications (now Broadband Infocommunications and Electromagnetic Theory) in 1986, where he is currently an associate professor. He is a lecturer on graduate and postgraduate courses at BME on Antennas and radiowave propagation, Radio system design, Adaptive antenna systems and Computer Programming. His research interests include antenna analysis and computer aided design, electromagnetic theory, radiowave propagation, communication electronics, signal processing and digital antenna array beamforming, topics where he has produced more than 100 different book chapters and peer-reviewed journal and conference papers. Member of Hungarian Telecommunication Association, official Hungarian Member and Hungarian Committee Secretary of URSI, Chair of the IEEE Chapter AP/ComSoc/ED/MTT.